

# Synthesis and reaction kinetics for monodispersive $Y_2O_3:Tb^{3+}$ spherical phosphor particles

J.M. Sung, S.E. Lin, W.C.J. Wei\*

*Department of Material Science and Engineering, National Taiwan University Taipei 106, Taiwan, ROC*

Received 15 June 2006; received in revised form 28 October 2006; accepted 3 November 2006

Available online 5 January 2007

## Abstract

Monodispersive  $Y_2O_3:Tb^{3+}$  spherical phosphor was synthesized by homogenous precipitation process. By using X-ray diffractometer, thermogravimetric analysis (TGA), transmission and scanning electron microscopes, and inductively coupled plasma (ICP)-optical emission spectrometry (OES), the precipitation behaviors were analyzed. The results indicated that the kinetics of the hydrolysis reaction of  $Y^{3+}$  and  $Tb^{3+}$  was a zero-order reaction, controlled by the decomposition of urea with an activation energy of 131 kJ/mol. Besides, the effect of urea concentration, reaction temperature, and aging time for the control of the precipitate size were also investigated. The dopant  $Tb^{3+}$  in the solution did not significantly influence the precipitation of the yttrium component. After 800 °C calcination, the  $Y_2O_3:Tb^{3+}$  powder showed nano-crystalline characteristics and emitted strong green light by a UV excitation light source.

© 2006 Elsevier Ltd. All rights reserved.

**Keywords:**  $Y_2O_3$ ; Phosphor

## 1. Introduction

Phosphors play an important role in display applications. Among all phosphors, yttria ( $Y_2O_3$ ) is a well known host material which has been widely used in cathode radiation tube (CRT), field emission display (FED), and thin film electroluminescence (TFEL) devices.<sup>1</sup> According to previous studies, yttria doped with specific rare earth elements or materials shows interesting photoluminescent (PL) and electroluminescent (EL) properties.<sup>2,3</sup> In addition to the optical properties, yttria has a high melting point (2698 K) with excellent chemical stability and low volatility in vacuum.

Traditional processes for synthesis of phosphors are mainly divided into two methods: solid-state reaction and wet-chemical process. The former method is popular for commercial production of phosphors. However, solid-state reaction may experience the contaminations from ball milling or non-well-mixed dopant (second phase). Irregular morphologies and wide size distribution are non-favorable for the phosphor powders obtained by such solid-state reaction.<sup>4</sup>

Instead of solid-state reaction, wet-chemical process is considered better for its molecular level mixing. Molecular level mixing offers the possibilities for controlling the chemical composition, obtaining better homogeneity, single phase, and higher surface area powder.<sup>4,5</sup> Generally, wet-chemical processes refer to homogeneous precipitation method, hydrothermal method, and sol-gel method. Irregular shape and agglomerated powder was obtained often from sol-gel method.<sup>4</sup> Among all wet-chemical processes, homogenous precipitation has the advantage of generating fine particles with relatively narrow size distribution compared to others. And it is also considered the best process for the ability to control the morphology of the precipitates.

When a specific type of organic compound, e.g., urea,<sup>6</sup> slowly decomposes in the solution which contains metal cations, the generated anions will combine with metal cations and form the precipitation nuclei. By adjusting the concentration of reactants, pH value of the solution, reaction temperature, and reaction time, we can easily control the concentration of nuclei and the growth rate of the precipitates. That means we can control the morphology, size, and size distribution of the precipitates.<sup>7,8</sup> For example, Boschini et al.<sup>9</sup> prepared nano-sized barium zirconate powder by thermal decomposition of urea in an aqueous solution containing  $Ba^{2+}$  and  $Zr^{4+}$ . Another case was reported by Lin

\* Corresponding author. Tel.: +886 2 23632684; fax: +886 2 23634562.  
E-mail address: [wjwei@ntu.edu.tw](mailto:wjwei@ntu.edu.tw) (W.C.J. Wei).

and Wei<sup>10</sup> who synthesized oval, stick, and cubic-shaped indium oxide powders with the help of urea. Both cases are based on homogenous precipitation of metal cations with anions from the decomposition of urea.

Monodispersive and spherical particles have many potential and important applications, e.g., for the manufacture of photonic bandgap crystals or as model materials for fundamental studies in colloidal and surface science.<sup>8</sup> Besides, theoretically, owing to the high surface area for monodispersive spherical particle, the efficiency should be better for a phosphor with this kind of morphology. In this study, spherical Y<sub>2</sub>O<sub>3</sub>:Tb particles have been synthesized by the homogenous precipitation method. We discuss the precipitation behavior with different aging time, temperature and urea additions. The reaction kinetics of the hydrolysis reaction of Y<sup>3+</sup> and Tb<sup>3+</sup> cations at the temperature 65–85 °C is investigated in this work.

## 2. Experimental procedure

### 2.1. Materials

Yttrium chloride (YCl<sub>3</sub>, 99.9% pure, Beyoung Chemical Corp., Ltd., China), terbium nitrate (Tb(NO<sub>3</sub>)<sub>3</sub>, 99.9% pure, Alfa Aesar, A Johnson Matthey, USA), and urea ((NH<sub>2</sub>)<sub>2</sub>CO, 99.5% pure, Acros, Geel, USA) were used for the preparation of Y<sub>2</sub>O<sub>3</sub>:Tb spherical particles.

### 2.2. Sample preparation

The solution concentration of YCl<sub>3</sub> was kept at 0.009 mol/L, Tb(NO<sub>3</sub>)<sub>3</sub> at 1.7 × 10<sup>-4</sup> mol/L, and the urea concentrations adjusted from 0.25 to 1 mol/L. The formulation and experimental condition are shown in Table 1. First, the urea was dissolved in de-ionized water, and then added to the diluted YCl<sub>3</sub> and Tb(NO<sub>3</sub>)<sub>3</sub> solution. Second, the mixture was sealed in a glass jug and aged at the specific temperature. Finally, after aging the mixture for a specific period, the precipitate in the solution was separated by centrifugation for 30 min at 5000 rpm and the supernatant solution was discarded. This centrifuging treatment was repeated at least three times. For each cycle, the centrifuged particles were re-dispersed in de-ionized water.

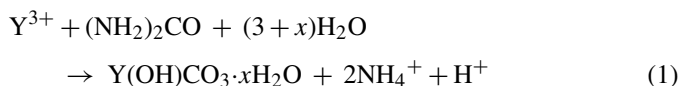
### 2.3. Characterization

After the first centrifuging, the supernatant was collected for inductively coupled plasma (ICP)-optical emission spectrometry (OES) measurement. And the separated powder was dried at 105 °C for more than 2 h. About 10 mg of the powder sample was placed in a Pt crucible and tested in the thermogravimetric analysis (TGA) system (Thermal Gravity Analyst 2000, Dupont Co., Wilmington, DE, USA); 5 mg of the sample powder was spread on a fillister in a black box and then measure the photoluminescent property directly by FL2006 (Labguide, Co., Ltd., USA) under a 254 nm ultraviolet excitation light source. The particle size and morphology were examined by scanning and transmission electron microscopes (Field Emission SEM with EDS, LEO 1530, Cambridge, UK; TEM 100 CX II, JEOL Co., Tokyo, Japan). The crystalline phase was examined by X-Ray diffractometry (XRD, Philips PW1710, Philip Co., Eindhoven, The Netherlands). The particle size was statistically measured from the SEM micrographs based on at least 300 particles.

## 3. Results and discussion

### 3.1. Hydration reactions

According to Aiken et al.<sup>5</sup>, homogenous precipitation reaction mechanism for yttrium precipitate can be classified in three steps. The overall chemical reactions can be described as follows:



The above equation shows that one mole of urea would react with one mole of yttrium cations to form an equi-molar yttrium compound (Y(OH)CO<sub>3</sub>·1H<sub>2</sub>O). Accordingly, the pH value of the solution will decrease due to the generation of protons as the reaction proceeds.

In fact, the variation of pH value versus aging time in Fig. 1 can be divided into three stages. In the first stage (for sample Y-3 was 0–1 h), the pH value increased with aging time. This phenomenon was caused by the decomposition of urea and the release of OH<sup>-</sup> anions into the solution. In the second stage (for sample Y-3 was 1–5 h), the pH value tended to slightly decrease due to the hydrolysis reaction of Y<sup>+3</sup>, as shown in Eq. (1). The

Table 1  
Formulation and experimental conditions used in this study

Sample	[Y <sup>3+</sup> ] (mol/L)	[urea] (mol/L)	[Tb <sup>3+</sup> ] (mol/L)	Reaction temperature (°C)	Longest aging time (h)
Y-1	9.0 × 10 <sup>-3</sup>	0.5	1.7 × 10 <sup>-4</sup>	65	24
Y-2	9.0 × 10 <sup>-3</sup>	1.0	1.7 × 10 <sup>-4</sup>	65	20
Y-3	9.0 × 10 <sup>-3</sup>	0.25	1.7 × 10 <sup>-4</sup>	75	7
Y-4a	9.0 × 10 <sup>-3</sup>	0.5	1.7 × 10 <sup>-4</sup>	75	7
Y-4b	9.0 × 10 <sup>-3</sup>	0.5	0	75	7
Y-5a	9.0 × 10 <sup>-3</sup>	1	1.7 × 10 <sup>-4</sup>	75	5
Y-5b	9.0 × 10 <sup>-3</sup>	1	0	75	5
Y-6	9.0 × 10 <sup>-3</sup>	0.25	1.7 × 10 <sup>-4</sup>	85	5
Y-7	9.0 × 10 <sup>-3</sup>	0.5	1.7 × 10 <sup>-4</sup>	85	4

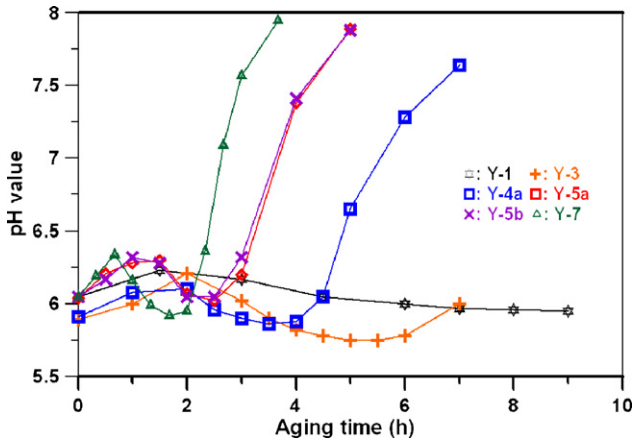


Fig. 1. pH value of the solutions in this study plotted against the aging time.

ICP-OES data revealed that the concentration of  $Y^{3+}$  cations in the solution decreased (over-saturated) in the second stage and the solution became turbid. The nuclei of the precipitate started to grow in this stage. Finally, in the third stage (for sample Y-3 was longer than 5 h), the pH value increased again. This was because of the complete reaction of the cations in the solution to form the precipitate. However, the residual urea would keep on decomposing and release  $OH^-$ , which resulted in increasing the pH value.

### 3.2. Precipitation kinetics

Fig. 2 shows the ICP-OES results of the residual concentration of  $Y^{3+}$  and  $Tb^{3+}$  cations in the solution plotted against the aging time. As for  $Y^{3+}$  cations (Fig. 2(a)), in the case of sample Y-3, the  $[Y^{3+}]$  is constant for aging in 2 h and almost used up when aging time is longer than 7 h. Moreover, it also provided the evidence that, after aging for longer than 7 h, the particle size would remain constant throughout the reaction, which we will discuss later. Similar situations were observed for other cases.  $[Y^{3+}]$  is almost constant for a few hours of the reaction and then falls to  $2 \pm 1$  ppm level when aged for 20, 5, 4, 4, and 3 h for Y-1, Y-4a, Y-5a, Y-5b, and Y-7 cases, respectively. It was noticed that, in the cases of Y-5a and Y-5b, the addition of  $Tb^{3+}$  did not have any apparent influence on the precipitation of  $[Y^{3+}]$ .

The reaction of  $Tb^{3+}$  cations in solution is similar to that of  $[Y^{3+}]$ , as shown in Fig. 2(b). However, according to the results of ICP-OES, we found that the initial precipitation point for  $[Tb^{3+}]$  was about half an hour earlier than for  $[Y^{3+}]$ . This may be due to a lower solubility of  $Tb^{3+}$  cations in the solution. Therefore,  $[Tb^{3+}]$  reached the over-saturated point half an hour earlier than  $[Y^{3+}]$  cations to precipitate. This phenomenon did not cause a serious problem for the “co-precipitation” of  $[Tb^{3+}]$  with  $[Y^{3+}]$  during the synthesis.

After fitting the ICP-OES results, as shown in Fig. 2(a and b), a linear relationship between the concentration of the residual cations and the aging time of the solution could be obtained, in which the residual  $[Y^{3+}]$  and  $[Tb^{3+}]$  were higher than  $2 \pm 1$  ppm. For a zero-order reaction, the slope of the linear fitting line

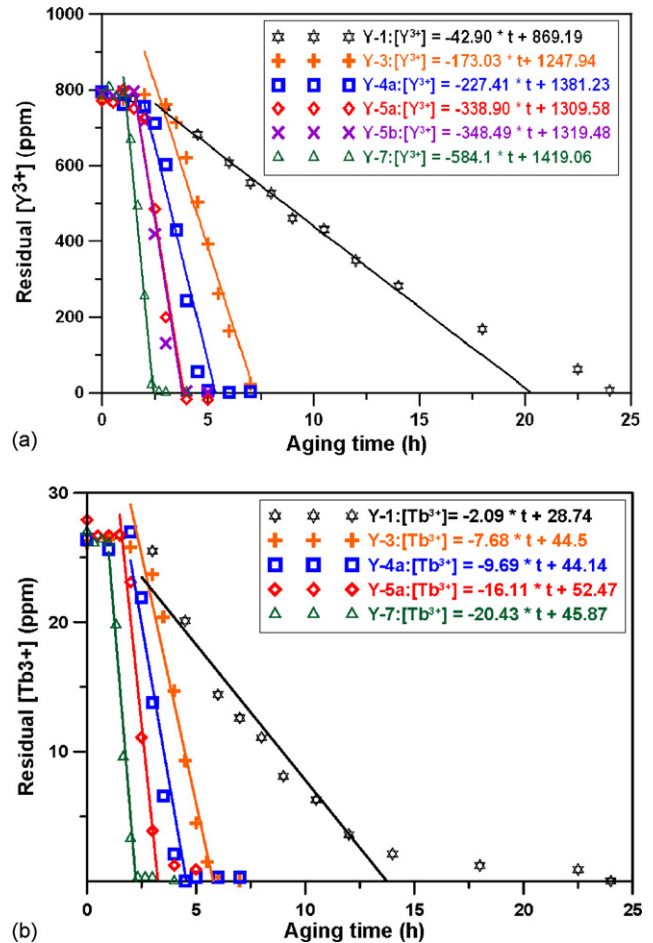


Fig. 2. Residual: (a)  $[Y^{3+}]$  and (b)  $[Tb^{3+}]$  in the solutions for specified conditions of this study, plotted against the aging time.

represents the reaction rates of the precipitate.

$$R = -\frac{d[C]}{dt} = k[C]^0 \quad (2)$$

where  $k$  is the reaction rate constant (ppm/h),  $R$  the reaction rate, and  $[C]$  is the concentration of cations ( $[Y^{3+}]$  or  $[Tb^{3+}]$  in this study) in solution.

From ICP-OES results, we can also find that as the reaction temperature changes from 65 to 85 °C, the hydrolysis reaction rate of  $Y^{3+}$  and  $Tb^{3+}$  increases with the increase of urea addition.

The slope of the reaction rate versus urea addition is defined as the reaction rate constant  $k$  and shown in Fig. 3. The values of reaction rate constants of 65, 75, and 85 °C were 38.8, 221.4, and 575.3, respectively. The difference of the three cases results from the different decomposition rates of urea at the specified temperatures.

The activation energy for the precipitation of yttrium compound can be considered as the energy required to overcome the energy barrier for the reaction. The reaction rate constant  $k(T)$  varies as a function of the reciprocal absolute temperature shows as below:

$$k(T) = k_0 \exp\left(\frac{-Q}{R_{\text{gas}}T}\right) \quad (3)$$

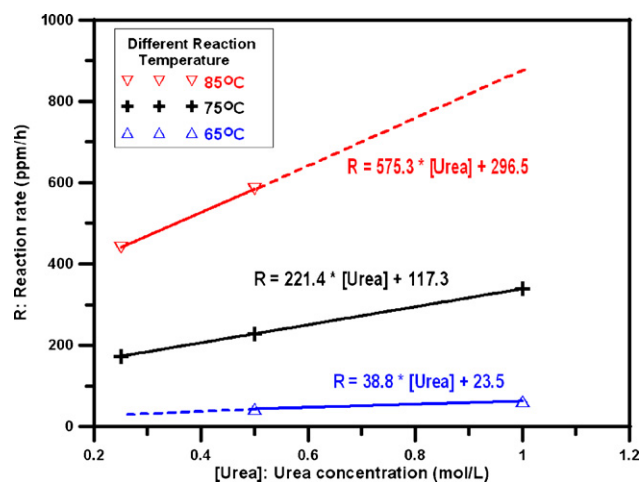


Fig. 3. The relationship between the reaction rate (ppm/h) of  $Y^{3+}$  cations and urea concentration.

where  $k_0$  is the pre-exponential factor, and  $R_{\text{gas}}$  the gas constant ( $J(\text{mol K})^{-1}$ ),  $T$  is in absolute or Kelvin units.

An Arrhenius plot of the reaction rate constant of 65, 75, and 85 °C is also shown in Fig. 4. Shaw and Bordeaux<sup>11</sup> reported the decomposition behavior of urea in aqueous solution at 65–100 °C. Recently, Lin and Wei<sup>10</sup> showed the reaction kinetics of  $[\text{In}^{3+}]$  with the decomposition of urea. The activation energy reported by Shaw ( $Q_1$ ) and by Lin ( $Q_2$ ) was about 128 and 133 kJ/mol, respectively. The activation energy for the precipitation of  $\text{Tb}^{3+}$  doped yttrium compound, denoted as  $Q$ , in this study was about 137 kJ/mol. Our result is in a good agreement with the reports of the others, implying that the factor controlling the mechanism of reactions in this study is indeed the decomposition of urea.

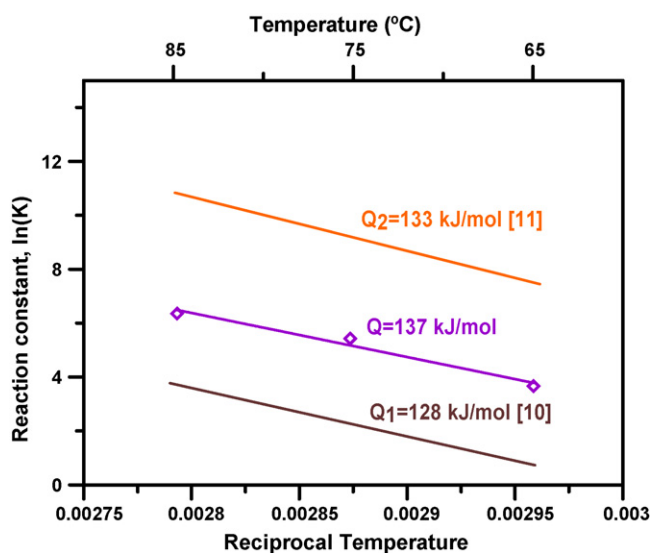


Fig. 4. Arrhenius plot of the reaction rate constant vs. the reciprocal Kelvin temperature. The activation energy for the decomposition of urea reported in literatures<sup>10,11</sup> was about 128 and 133 kJ/mol, respectively. The activation energy ( $Q$ ) for the precipitate of yttrium compound in this study is 137 kJ/mol.

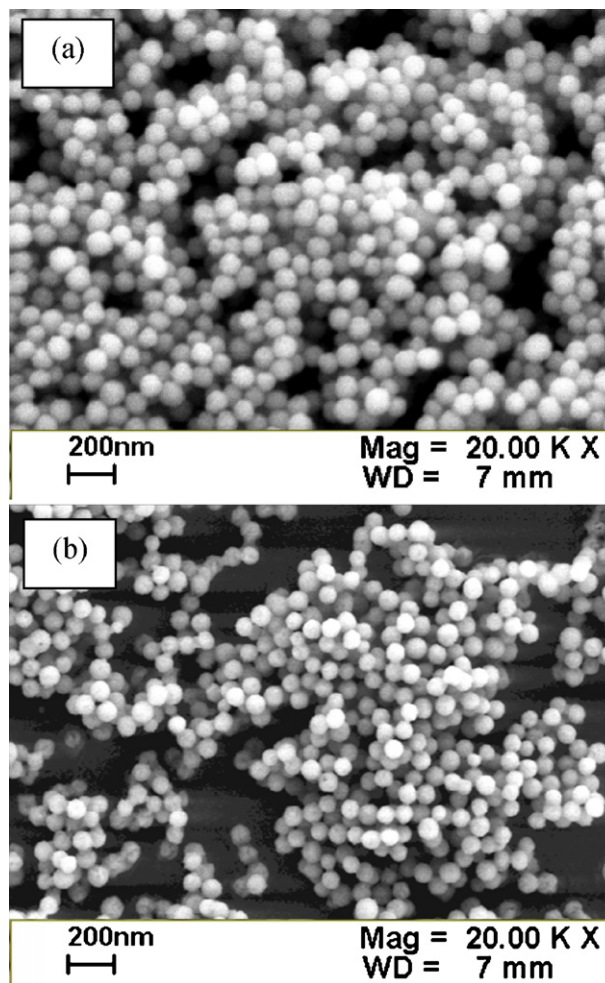


Fig. 5. SEM micrographs of the sample Y-4a (a) as-dried, (b) after calcination at 800 °C for 2 h. Aging time in the cases was 7 h.

### 3.3. Microstructural observation

Fig. 5(a and b) show the morphologies of the yttrium compounds with  $\text{Tb}^{3+}$  (samples Y-4a). SEM micrographs show that the morphology (size and shape) of the precipitation in both cases are similar. Size measurement indicated the average particle size would reduce from about 110 nm (as-dried) to 90 nm (as-calcined at 800 °C for 2 h) for the Y-4a sample. The as-prepared particles should be porous, but sintered to higher density by the calcination. Later, TEM results (Fig. 9) will be presented to reveal the interior of the calcined particles.

The effect of urea concentration versus the average particle size is shown in Fig. 6(a). It can be seen that the greater the urea concentration, the smaller the mean particle size, the more the nucleus density is generated in the solution per unit time. The high urea concentration would eventually lead to a smaller particle size.

Fig. 6(b) shows the variation of mean particle size of sample Y-4a versus the aging time during reaction period. In this case, up to 3 h of aging time, no obvious precipitate could be observed. However, the particle size grew from about 75 to 110 nm as the aging time increased from 3 to 5 h. The mean particle size

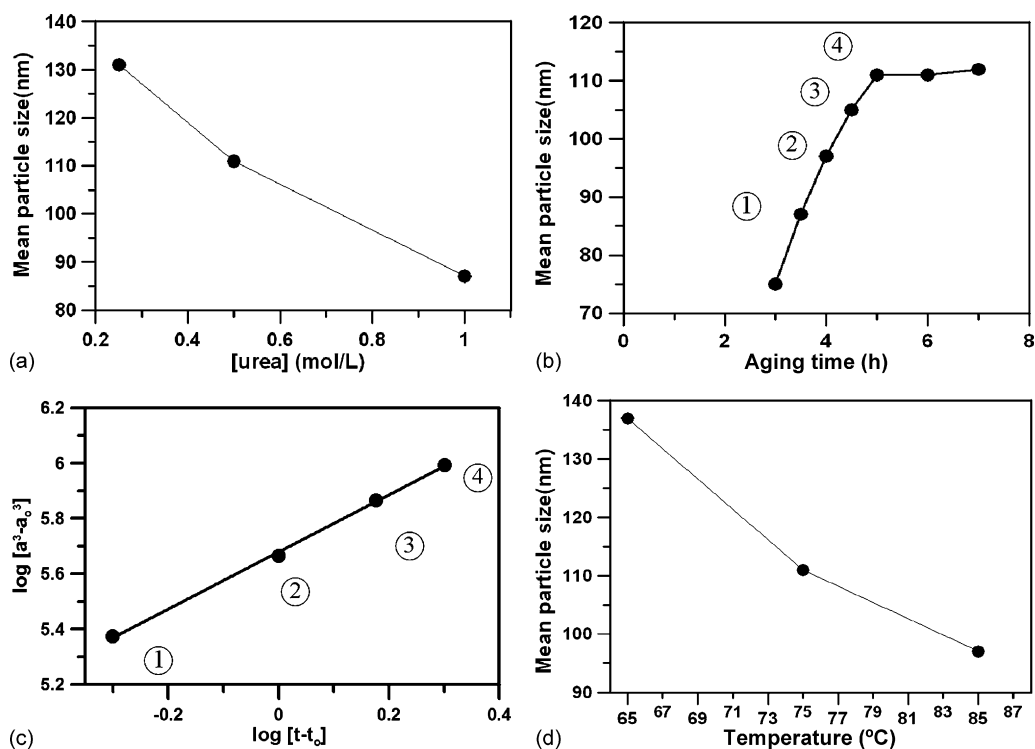


Fig. 6. Mean particle size plotted against (a) the urea concentration (after complete reaction of samples Y-3, Y-4a, and Y-5a), (b) the reaction time of Y4-a, (c) size variation  $[a^3 - a_0^3]$  vs. normalized aging time  $[t - t_0]$  plotted in log–log scale, (d) mean particle size vs. the reaction temperature (after complete reaction samples of Y-1, Y-4a, and Y-7). All of the samples reported here were measured in as-synthesized state.

remained constant when aged longer than 5 h. It resulted from the complete reaction of the  $[Y^{3+}]$  reactants (Fig. 2). The precipitate was no longer growing as holding for more than 5 h.

Fig. 6(c) shows the analysis results of the growth behavior shorter than 6 h. As the initial mean particle size  $a_0 = 75$  nm is taken, the growth kinetics ( $a^3 - a_0^3$ ) show a linear relationship between the normalized aging time ( $t - t_0$ ) in the log–log plot. The kinetics of this case performed an Ostwald ripening phenomenon,<sup>12</sup> of which the diffusion-limited growth of the precipitates in the system has the  $t^{1/3}$  time dependence.

The effect of reaction temperature versus mean particle size is shown in Fig. 6(d). As observed from the figure, the mean particle size is smaller at higher reaction temperature. A higher reaction temperature generates more nuclei at the beginning of the reaction.

Fig. 7 shows the X-ray diffraction results of completely reacted sample Y-4a as-dried and after calcination at 800 °C for 2 h. From the XRD spectra, the yttrium compound precipitate is amorphous before calcination, and it transformed to  $Y_2O_3$  crystalline phase after calcination. We have tried to find if the spectrum shifts after doping with  $Tb^{3+}$  in the sample. However, the size of the  $Y^{3+}$  and  $Tb^{3+}$  is 0.900 and 0.923 Å, respectively, when the coordination number is 6.<sup>13</sup> The difference between those two ions is less than 3%. As a result, the peak shift of the X-ray spectrum is hardly observed.

EDS analysis on randomly selected particles of the above sample is shown in Table 2, which lists five measurements. The average content of  $Tb^{3+}$  solid solution in  $Y_2O_3$  is 5.0 at.%, and appear a concentration variation of 0.45 at.% in a 90% confi-

dence. The  $Tb^{3+}$  dopant distributes in every synthesized particles with the concentration enough for PL emission.

TGA results (Fig. 8) show that the mass of sample Y-4a remains constant after calcining to the temperatures higher than 650 °C. It reveals the fact that the phase transformation from amorphous yttrium compound to yttria finishes at 650 °C. A

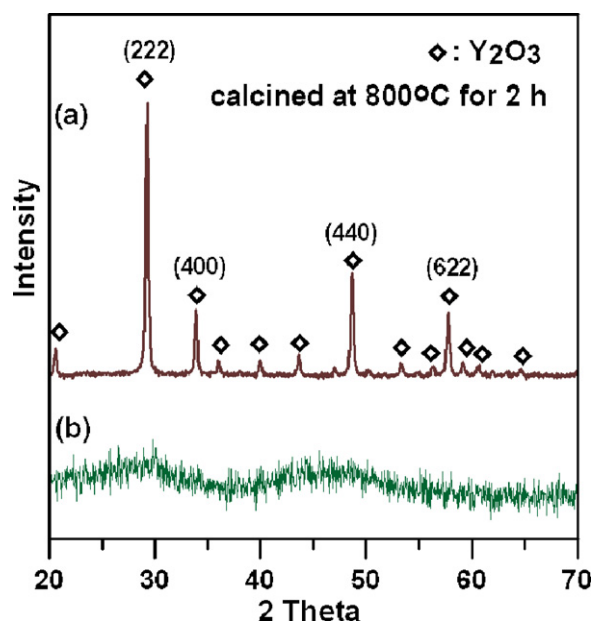


Fig. 7. XRD results of sample Y-4a (a) as-dried and (b) after calcination at 800 °C for 2 h. Aging time in this case was 7 h.

Table 2  
Semi-quantitative EDS analysis results of sample Y-4a

EDS	Y/Tb (wt.%)	Y/Tb (at.%)
1	92.2/7.8	95.5/4.5
2	91.9/8.1	95.3/4.7
3	91.7/8.3	95.2/4.8
4	91.1/8.9	94.8/5.2
5	90.3/9.7	94.3/5.7
Average	91.4/8.6	95.0/5.0

complete transformation would take place after calcining at 800 °C for 2 h. The TGA result also reveals that about 35–45% mass loss is resulted after the transformation, which is close to the theoretical mass loss (39%) by Eq. (1). The discrepancy of mass loss from sample to sample may be due to the residual water containing in the samples. If the mass loss between 220 and 700 °C was measured, the loss percentage was 33%, which is close to the conversion loss (32%) of  $Y(OH)CO_3$  to  $Y_2O_3$ . Their DTA results are similar, basically showing one endothermic peaks at 200–400 °C, one exothermic at 450–700 °C. The peaks represents the dehydration of the sample and the decomposition of Y-carbonate to  $Y_2O_3$ , respectively.

The variation of the precipitate morphology and size distribution of sample Y-4a before and after calcination (heating rate: 5 °C/min, at 800 °C for 2 h) are shown in Fig. 9, which shows the TEM micrographs of the microstructure of the Y-4a particles after calcination (heating rate: 5 °C/min, at 800 °C for 2 h). From Fig. 9(a), some nanopores present in the particles can be observed, as shown by the arrows. The pores can be the residue of incomplete sintering, or induced by trapped water, or resulted by in-appropriate calcination schedule for the transformation of the yttrium compound to oxide. Besides, thickness fringes on the particles were observed. Since the particle size was smaller than the spot size of the electron beam, we could only get the ring pattern of these particles. After indexing, the grains were in the crystalline yttria phase, as shown in Fig. 9(b).

Furthermore, in order to confirm the crystallinity of the yttria particles, center dark field (CDF) mode was used in this analysis. From Fig. 9(c and d), which are the images of sample Y-4a in the BF or CDF mode, respectively, the yttria is polycrystalline in each individual particle.

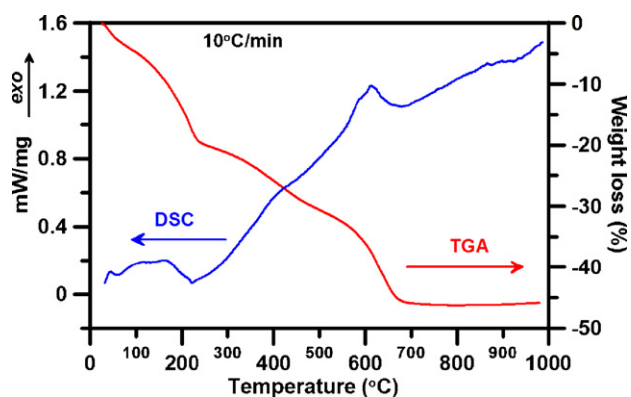


Fig. 8. TGA and DSC analysis of sample Y-1 (aging for 24 h). The heating rate was 10 °C/min.

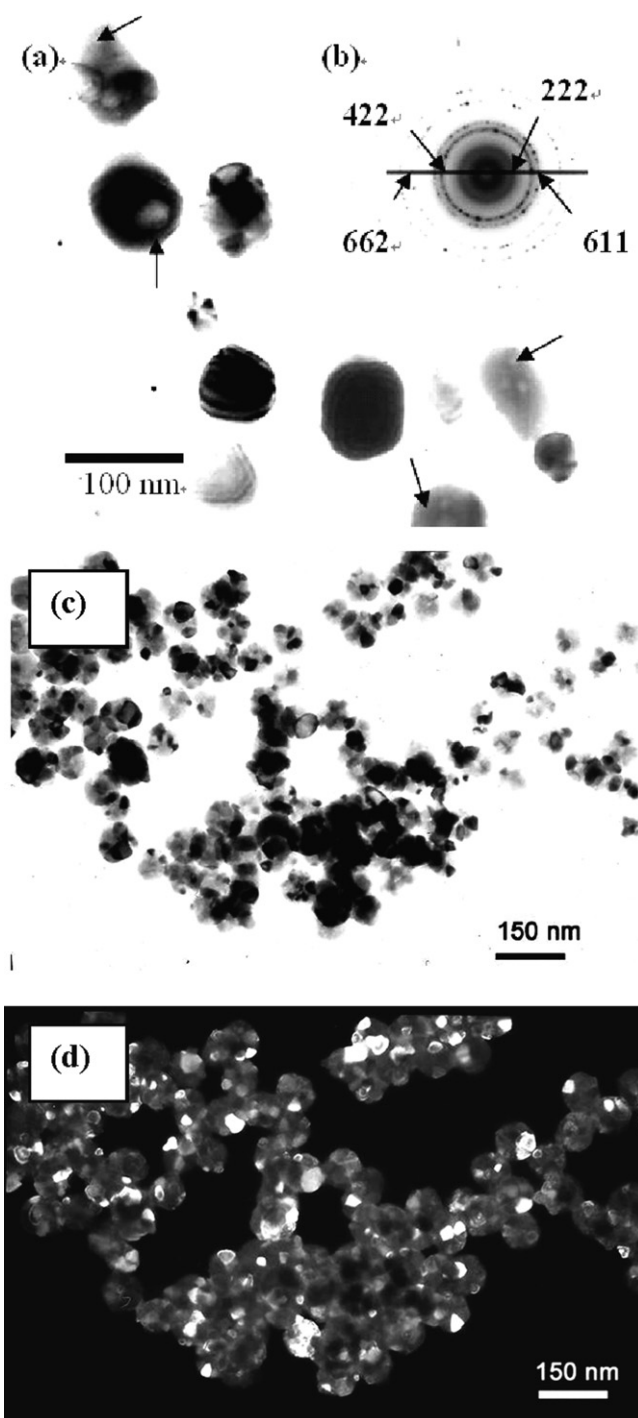


Fig. 9. (a) TEM BF micrograph (b) ring pattern of the particles of the Y-4a particles (heating rate: 5 °C/min, at 800 °C for 2 h). The arrows point out the micropores in the particles and the thickness fringes also could be found in some particles. The imaging of the Y-4a sample in (c) BF mode and (d) CDF mode, which was illuminated by (222)  $Y_2O_3$  diffraction intensity.

### 3.4. PL properties

Fig. 10 shows the result of PL spectrum for the sample Y-4a. The  $Tb^{3+}$  doped yttria emitted green light with a maximal intensity at 546 nm. The corresponding energy transition was from  $^5D_4$  to  $^7F_5$ , as shown in Fig. 10(a). However, Y-4b, yttria

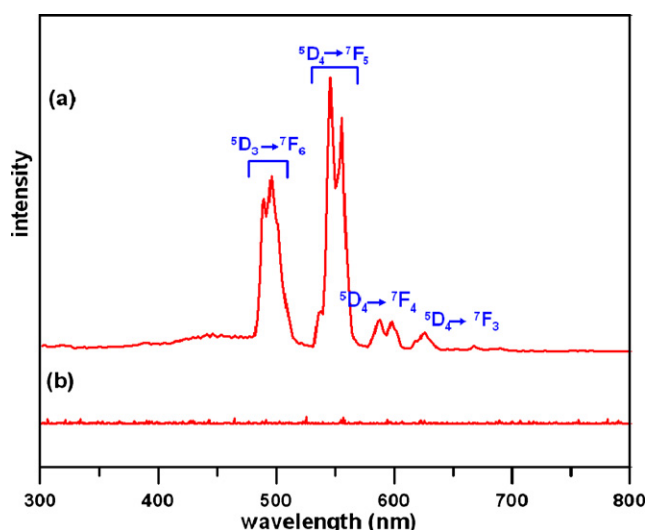


Fig. 10. PL spectra of calcined sample: (a) Y-4a and (b) Y-4b at 800 °C for 2 h.

without doping, did not show any PL spectrum peak, as shown in Fig. 10(b).

#### 4. Conclusions

The results of this work can be summarized as follows:

- (1) Monodisperse  $\text{Y}_2\text{O}_3:\text{Tb}^{3+}$  spherical phosphors were synthesized by homogenous precipitation at 65–85 °C with the addition of urea. The precipitation kinetics of  $\text{Y}^{3+}$  and  $\text{Tb}^{3+}$  cations in the solution were investigated. The results show a zero-order reaction which is controlled by the decomposition of the urea with an activation energy of 137 kJ/mol.
- (2) The size of the precipitates can be controlled by adjusting the concentration of urea, reaction temperature, and aging time of the solution. Besides, the results reveal that the doped  $\text{Tb}^{3+}$  in the solution has no obvious influence on the morphology of the yttrium-based precipitate.
- (3) The particles grow by the kinetics of Ostwald ripening in the stage of synthesis.
- (4) As for the results of TGA, DSC, and X-ray diffraction, the yttrium compound ( $\text{Y}(\text{OH})\text{CO}_3 \cdot \text{H}_2\text{O}$ ) is an amorphous phase which transforms to yttria ( $\text{Y}_2\text{O}_3$ ) crystalline phase after calcination at the temperatures higher than 650 °C.

SEM results show that the precipitate experiences shrinkage after 800 °C for 2 h of calcination. From TEM results, we have observed the existence of nanopores in the particles.

- (5)  $\text{Y}_2\text{O}_3:\text{Tb}^{3+}$  powder showed a strong green light (546 nm) PL emission under 254 nm UV light excitation.

#### Acknowledgements

This work was financially supported by National Science Council, under grant NSC93-2120-M-002-011. The authors thank the editing by Dr. K. Borgohain and valuable suggestions given by Professor C.F. Lin.

#### References

1. Kitai, A. H., Oxide phosphor and dielectric thin films for electroluminescent devices. *Thin Solid Films*, 2003, **445**, 367–376.
2. Minami, T., Oxide thin-film electroluminescent devices and materials. *Solid-State Electron.*, 2003, **47**, 2237–2243.
3. Wakefield, B. G., Holland, E. and Dobson, P. J., Luminescence properties of nanocrystalline  $\text{Y}_2\text{O}_3:\text{Eu}^{3+}$ . *Adv. Mater.*, 2001, **13**, 20.
4. Wuo, B. C., *Modification and characterization of strontium orthosilicate and yttrium oxide phosphors*, MS Thesis, National Taiwan University, 2005.
5. Aiken, B., Hsu, W. P. and Matijevic, E., Preparation and properties of monodispersed colloidal particles of lanthanide compounds: III, yttrium(III) and mixed yttrium(III)/cerium(III) system. *J. Am. Ceram. Soc.*, 1988, **71**(10), 845.
6. Sun, Y., Qi, L., Lee, M., Lee, B. I., Samules, W. D. and Exarhos, G. J., Photoluminescent properties of  $\text{YO}_3:\text{Eu}^{3+}$  phosphors prepared via urea precipitation in non-aqueous solution. *J. Lumin.*, 2004, **109**, 85–91.
7. Martinez-Rubio, M. I., Ireland, T. G., Silver, J., Fern, G., Gibbons, C. and Vecht, A., Effect of EDTA on controlling nucleation and morphology in the synthesis of ultrafine  $\text{Y}_2\text{O}_3:\text{Eu}^{3+}$  phosphors. *Electrochem. Solid-State Lett.*, 2000, **3**(9), 446–449.
8. Matijevic, E., Preparation and properties of uniform size colloids. *Chem. Mater.*, 1993, **5**, 412–426.
9. Boschini, F., Robertz, B., Rulmont, A. and Cloots, R., Preparation of nano-sized barium zirconate powder by thermal decomposition of urea in an aqueous solution containing barium and zirconium and by calcination of the precipitation. *J. Eur. Ceram. Soc.*, 2003, **23**, 3035–3042.
10. Lin, S. E. and Wei, W. C. J., Synthesis and growth kinetics of monodisperse indium hydrate particles. *J. Am. Ceram. Soc.*, 2006, **89**(2), 527–533.
11. Shaw, W. H. R. and Bordeaux, J. J., The decomposition of urea in aqueous media. *J. Chem. Soc.*, 1955, **77**, 4729.
12. Chiang, Y. M., Birnie III, D. P. and Kingery, W. D., *Physical Ceramics Principles for Ceramic Science and Engineering*. John Wiley & Sons, Inc., 1997, pp. 388–391.
13. <http://abulafia.mt.ic.ac.uk/shannon/ptable.php>.